



Encapsulation of organic active material in carbon nanotubes for application to high-electrochemical-performance sodium batteries

Journal:	<i>Energy & Environmental Science</i>
Manuscript ID	EE-ART-09-2015-002806.R1
Article Type:	Paper
Date Submitted by the Author:	20-Oct-2015
Complete List of Authors:	Kim, Jae-Kwang; Ulsan National Institute of Science and Technology (UNIST), School of Energy & Chemical Engineering Kim, Yongil; Ulsan National Institute of Science and Technology, School of Energy and Chemical Engineering Park, Seungyoung; Ulsan National Institute Science and Technology, Ko, Hyunhyub; Ulsan National Institute of Science and Technology, School of Energy and Chemical Engineering Kim, Youngsik; Interdisciplinary School of Green Energy, Ulsan National Institute of Science and Technology, Ulsan (UNIST), Ulsan, Korea,



Journal Name

ARTICLE

Encapsulation of organic active material in carbon nanotubes for application to high-electrochemical-performance sodium batteries

Received 00th January 20xx,
Accepted 00th January 20xx

DOI: 10.1039/x0xx00000x

www.rsc.org/

Jae-Kwang Kim,^a*† Yongil Kim,^b† Seung-Young Park,^b Hyunhyub Ko,^b and Youngsik Kim^b*

Sodium batteries are an interesting candidate for replacing lithium batteries, primarily due to the abundance of sodium in the environment. However, the performance and energy density of a sodium battery are inferior to those of a lithium battery. Organic active materials can help overcome the drawbacks associated with sodium batteries because of their many advantages. However, such organic polymer electrodes are subject to a high self-discharge and low practical capacity because the polymer electrode easily dissolves in an organic electrolyte and forms an insulating layer. Therefore, in this study, we have designed a unique organic electrode in which an active polymer is encapsulated in a carbon nanotube (CNT) to form an electrode with high polymer content. The CNT is able to retain the active polymer within the electrode structure, providing an effective electronic conduction path. Moreover, the CNT can contain large amounts of active polymer and therefore exhibits superior electrochemical properties without self-discharge, making it well suited to use as a cathode material in a sodium battery.

Introduction

Rechargeable lithium batteries have been widely adopted as power sources for portable electronic devices such as smart phones, laptop computers, and tablets because of their high energy density and long cycle life. Their range of application has been expanded to large-scale energy storage for electric vehicles (EVs) and energy storage systems (ESS).¹⁻³ However, against this large-scale demand for lithium batteries, we have to consider the increasing cost of lithium because of the limited quantities available to mine in the Earth's crust.

Sodium batteries are an interesting candidate for replacing lithium batteries, primarily due to the abundance of sodium in the environment. Therefore, they are attracting considerable attention as large-scale electrical energy storage systems.^{4,5} The main component of such a battery is the sodium intercalation-type inorganic cathode, which determines the battery's energy density and capacity. The performance of a sodium battery is inferior to that of a lithium battery because of the large ionic radius of the Na ions and the slow reaction kinetics.⁶⁻⁸ Moreover, a sodium battery will typically exhibit a lower energy density than a lithium battery owing to its relatively large weight and the low reduction potential of sodium.^{6,7}

Organic active materials offer the promise of solving the drawbacks of sodium batteries because they have some inherent advantages such as their lightness, fast reaction kinetics, renewability, and environmental-friendliness. Furthermore, they are abundant resources with a high electrochemical reaction constant.⁹⁻¹¹ Among the organic active materials, poly(2,2,6,6-tetramethylpiperidinyloxy-4-vinylmethacrylate) (PTMA) has a stable organic radical 2,2,6,6-tetramethyl-1-piperidinyloxy (TEMPO) as its repeating unit, which exhibits a fast reversible oxidation/reduction behavior and which allows higher levels of power, high potentials, and a long cycle life.¹²⁻¹⁴ The nitroxide radical moiety of the initial state TEMPO is oxidized to an oxoammonium cation during charging. During discharging, the oxoammonium cation is reduced to a nitroxide radical and aminoxy anion by means of a two-stage process.^{15,16} In the subsequent electrochemical process, the TEMPO radical exhibits a two-electron redox reaction, corresponding to a theoretical capacity of 225 mAh g⁻¹, while the reversible electrochemical reaction occurs rapidly with the anions/cations of the electrolyte, as shown in Fig. 1. The PTMA undergoes rapid redox reactions with an electron transfer rate constant in the order of 10⁻¹ cm s⁻¹, resulting in a high rate capability. However, the PTMA electrode is subject to a high self-discharge because the polymer electrode easily dissolves in an organic electrolyte.¹⁷⁻¹⁹ In addition, PTMA exhibits a low energy density due to its high insulating characteristics that give rise to a need for large amounts of carbon conductor in the electrode. When a high content PTMA of over 50 wt.% is applied to the electrode, the polymer battery exhibits inferior electrochemical properties because of the poor contact between the active polymer and carbon conductor.²⁰

^a Department of Solar & Energy Engineering, Cheongju University, Cheongju, Chungbuk 360-764, Republic of Korea. E-mail: jaekwang@cju.ac.kr

^b School of Energy & Chemical Engineering, Ulsan National Institute of Science and Technology (UNIST), 689-798 Ulsan, Republic of Korea. E-mail: ykim@unist.ac.kr

† These authors contributed equally to this work.

Electronic Supplementary Information (ESI) available:
See DOI: 10.1039/x0xx00000x

In this study, we designed a unique organic electrode, in which the active polymer is encapsulated in a carbon nanotube (CNT) to form a high-active polymer-content electrode. The CNT plays the role of a strong absorbent, retaining the active polymer material and preventing its dissolution into the electrolyte. The CNT also provides an effective electronic conduction path and their network-like structure forms a stable organic electrode structure. In addition, because the CNT provides a large surface area with a vacant space in the centre, it can contain of large amount of active polymer. Therefore, the organic electrode material encapsulated in the CNT exhibits superior electrochemical properties without self-discharge as a cathode material in a sodium battery, even with high active polymer content.

Experimental

Materials. PTMA was prepared by the radical polymerization of a 2,2,6,6-tetramethylpiperidine methacrylate monomer with a 2,2'-azobisisobutyronitrile initiator, followed by oxidation with hydrogen peroxide in the presence of a NaWO_4 catalyst (Fig. S9, ESI[†]) (purity $\geq 95\%$, and yield $\geq 85\%$).¹³ Carbon nanotube (CNT) with 120 nm average diameter was prepared by chemical vapor deposition (CVD).²¹ The PTMA was dissolved in CNT-containing N-methyl-2-pyrrolidone (NMP) solvent, where PTMA diffuses into the vacant spaces of the CNT. The PTMA-impregnated CNT was dried and washed in acetone, followed by vacuum filtering to remove excess PTMA on the outside of the CNT. The dissolution-diffusion-washing process was performed three times to produce well-impregnated CNTs (Fig. S1, ESI[†]). The cathode was prepared by blending the PTMA-impregnated CNT (93 wt.%) and poly(vinylidene fluoride) (PVdF) binder (7 wt.%). For comparison, we also fabricated a PTMA-CNT composite electrode using 63 wt.% PTMA, 30 wt.% CNT, and 7 wt.% PVdF. The length of the CNT ranges between 3 and 10 μm with an average length of 5 μm , while the diameter ranges between 100 and 300 nm.

Characterization of Morphology and Physical Properties of PTMA-impregnated CNT Electrode. Scanning electron microscopy (SEM) imaging and energy dispersive X-ray (EDX) mapping were performed using a Nanonova 230 scanning electron microscope (FEI, USA). Focused ion beam (FIB) measurements using a Quanta 3D FEG (FEI, USA) were performed to observe the inside of a CNT and PTMA-impregnated CNT. The size distribution of the PTMA-impregnated CNT was observed by high-resolution transmission electron microscopy performed using a JEM-3010 JEOL. Ab-initio Harree-Fock (HF) self-consistent field (SCF) molecular orbital calculations have been performed for the size of PTMA using the standard 6-31G* basis set.

Characterization of Electrochemical Performance. A PTMA-based sodium battery cell was fabricated by stacking a 300-mm sodium metal anode (Cyprus Foote Mineral Co.) and an organic cathode with a Celgard 2200 separator. The weight and thickness of PTMA-impregnated CNT electrode without Al substrate were 2.5 mg and 30 μm . The electrolyte was a 1M solution of NaClO_4 in ethylene carbonate/diethyl carbonate (1:1 v/v) (PanaXetec. Co.). The cell was assembled in an argon-filled glove box in which the moisture level

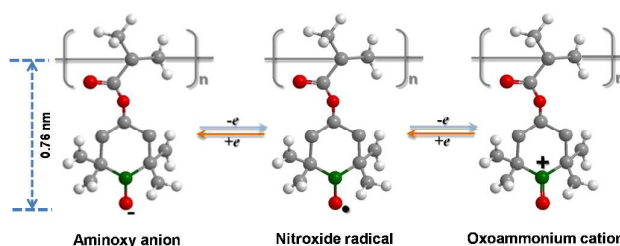


Fig. 1 Schematic representation of the electrochemical mechanism for PTMA.

was < 10 ppm. Electrochemical performance tests were carried out between 1.5 and 4.0 V at different current densities from 0.1 C to 5 C using a WBCS3000 battery tester (WonATech. Co.).

Results and discussion

A schematic diagram for the preparation of PTMA-impregnated CNT is shown in Fig. S1 (ESI[†]), and the details of the procedure are provided in the experimental section. The good thermal stability and weight percentage of PTMA-impregnated CNT is revealed by TGA analysis (Fig. S2, ESI[†]). An initial decomposition of PTMA occurs at 330 $^{\circ}\text{C}$ and 68 wt.% of PTMA in PTMA-impregnated CNT is disappeared at 500 $^{\circ}\text{C}$. The dried CNT of 32 wt.% is maintained to 600 $^{\circ}\text{C}$, which mean the weight percentages of the 68 wt.% PTMA and 32 wt.% CNT in the completed PTMA-impregnated CNT.

Fig. 2 shows focused-ion beam (FIB) images of a CNT and a PTMA-impregnated CNT. The CNTs are cut at a point 500 nm from the top to observe the inside of the CNT. The vacant space in the center of the CNT is clearly visible in Fig. 2a, while it can be seen that there is no empty space in the PTMA-impregnated CNT (Fig. 2b). Fig. 2d shows the results of EDX line-scanning across a cross-section of the PTMA-impregnated CNT (indicated by the solid red line in Fig. 2c). The red and green spectra represent the oxygen (O) and nitrogen (N) signal counts along the solid line, respectively. The EDX spectra prove the existence of PTMA in the CNT and the consistent signal indicates that the PTMA is uniformly distributed. The surface areas of the CNT and PTMA-impregnated CNT are determined by the BET method as presented in Fig. S3 (ESI[†]). The CNT exhibits an extremely large surface area of 122.1 $\text{m}^2 \text{g}^{-1}$ that corresponds to the unique tube morphology shown in the FIB image of Fig. 2a. In the PTMA-impregnated CNT, the surface area is significantly reduced to 11.6 $\text{m}^2 \text{g}^{-1}$, indicating that the CNT is completely filled with the PTMA. This is verified from the TEM/ FIB images of Fig. 2b and 2f. High-resolution transmission electron microscopy (HR-TEM) images of the CNT and PTMA-impregnated CNT, shown in Fig. 2e and f, respectively, clearly demonstrate that the vacant space inside the CNT (Fig. 2e) is filled by the PTMA. PTMA appears darker under TEM as it is heavier than the CNT. The red line in Fig. 2f corresponds to the EDX count for the carbon (C) signal, which is evenly distributed within the CNT. The spectrum shows that PTMA is present only inside the CNT and not on the outside.

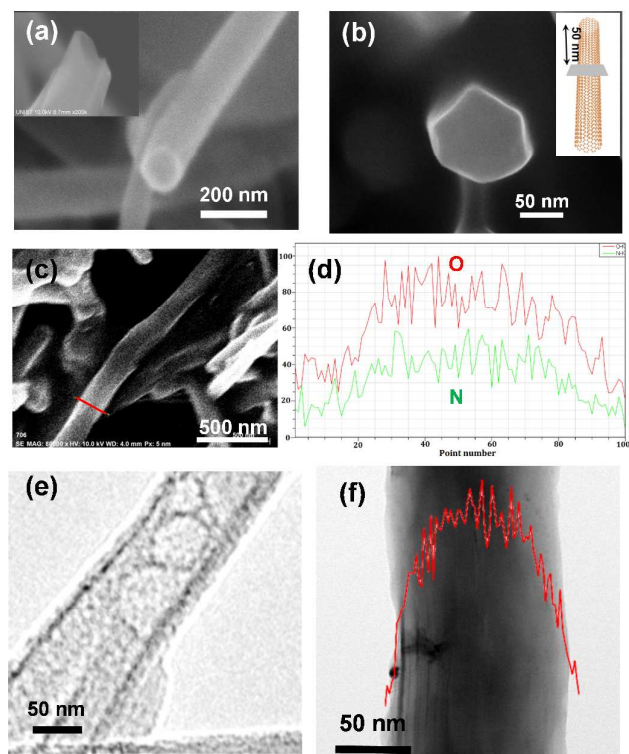


Fig. 2 FIB images of CNT (a) and PTMA-impregnated CNT (b), SEM image (c) and EDX line profile (d) of PTMA-impregnated CNT and TEM images of CNT (e) and PTMA-impregnated CNT (f) with EDX line scanning of C atom along the cross section.

To fabricate the general cathode, the PTMA and CNT were dissolved in NMP solvent to make slurry, followed by the usual process for preparing an electrode. In this process, the rod-like CNTs become coated with an insulating layer of PTMA. In fact, at a high PTMA content (> 60 wt.%), the electrode becomes non-conducting because the insulating PTMA perfectly surrounds the conductive CNT, as shown in Fig. S4 (ESI[†]). The thick layers of polymer coating tend to fuse together to produce a flake-like structure similar to that formed by pure PTMA.²⁰ The PTMA-CNT composite electrode exhibits a smooth surface due to the formation of a thick PTMA coating (Fig. 3a), which results in the ion exchange during the electrochemical reaction being mainly induced on the surface of the electrode. This is because the ions slowly diffuse to the inner part of the electrode due to the non-conducting nature of the electrode, while electron transfer is inhibited by the insulating PTMA layer between the CNTs. In contrast, the PTMA-impregnated CNT electrode has a three-dimensional morphology with an uneven surface, as shown in Fig. 3b, which results in easy electrolyte penetration and rapid ion diffusion in a sodium battery. Moreover, the direct contact between CNTs improves the electron transfer due to the reduced resistance.²²⁻²⁵ To understand the effect of the electrode surface morphology on the interface resistance and ion diffusion, impedance measurements were carried out, as shown in Fig. 3c. The medium-frequency semicircles are attributed to the charge-transfer resistance (R_{ct}) between the active polymer and electrolyte, while the low-frequency region corresponds to the ion diffusion process within the

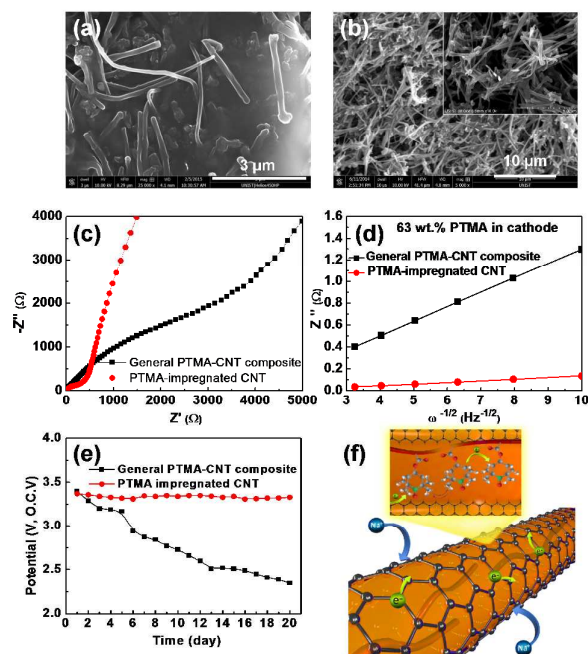


Fig. 3 SEM images of PTMA-CNT composite (a) and PTMA-impregnated CNT (b) electrodes, impedance spectra (c) and the relationship (d) between Z'' and square root of frequency ($\omega^{-1/2}$) in the low-frequency region for PTMA-CNT composite and PTMA-impregnated CNT electrodes. Open circuit voltage (OCV) (e) of a PTMA-CNT composite and PTMA-impregnated CNT based sodium batteries during twentieth days and (f) schematic illustration of PTMA-impregnated CNT structure.

electrodes.^{26,27} The charge-transfer resistance (R_{ct}) values of 3716 Ω and 283 Ω relate to the ion movement obtained for a general PTMA-CNT composite electrode and PTMA-impregnated CNT electrode, respectively. It is assumed that the thick, non-conducting PTMA layer in the PTMA-CNT composite electrode adversely affects the free passage of ions by functioning as a barrier at the electrode/electrolyte interface, thus resulting in a higher R_{ct} . Fig. 3d shows the relationship between Z'' and $\omega^{-1/2}$ ($\omega = 2\pi f$) in the low-frequency region. The low slope of the PTMA-impregnated CNT electrode in the low-frequency region indicates good ion kinetics in the electrode material.²⁶⁻²⁸ The general PTMA-CNT composite electrode exhibits a slope that is five times steeper than that exhibited by the PTMA-impregnated CNT electrode. The results of the impedance measurement suggest that the PTMA-impregnated CNT reduces the charge transfer resistance between the PTMA and electrolyte and improves the ion kinetics of the electrode.

Self-discharge rate is one important property of a rechargeable sodium battery and determines the lifetime and efficiency of the battery;^{17,19} a high self-discharge rate greatly decreases the lifetime and efficiency of the battery. The self-discharge effect arises from the dissolution of the active electrode material and is investigated from the change in the open-circuit-voltage (OCV), as shown in Fig. 3e. The Na cells are charged to a 100% state-of-charge (SOC) and the OCV is observed under conditions of no current flow. The OCV of the PTMA-impregnated CNT cell remains stable at 3.3 V over 20 days,

whereas that of the general PTMA-CNT composite decreases continuously, dropping to 2.3 V after 20 days.

The results indicate that the use of PTMA-impregnated CNTs effectively prevents the dissolution of organic active material, thereby minimizing self-discharge. Importantly, the narrow windows (or pores) of the CNT can trap PTMA during cycling due to the strong adsorption force between the graphene wall of the CNT and the PTMA, thus preventing the dissolution of the organic PTMA.²⁹⁻³² The TGA patterns in the bare PTMA and PTMA-impregnated CNT are an effective indication of the PTMA absorption strength in the carbon structure. The TGA curves for the bare PTMA (Fig. S5, ESI[†]) show that the PTMA evaporates at 240°C, but then its weight loss stops at 430°C. However, for the PTMA-impregnated CNT, the decomposition of the PTMA starts at 330°C, which is higher than that of pure PTMA. This indicates the existence of strong adsorption strength in the PTMA-impregnated CNT. The mechanism of electron transfer in the PTMA-impregnated CNT is shown in Fig. 3f. Heterogeneous electron transfer first occurs from the wall of the CNT to the TEMPO pendant (the stable organic radical that forms the repeating unit in PTMA), and then the electron is transferred to the neighboring TEMPO pendant by means of homogeneous electron transfer, which occurs as a result of a fast self-exchange reaction.³³ The electron self-exchange reaction between neighboring TEMPO pendants is a two-step electron process, involving conversion from aminoxy anions to oxoammonium cations, via a nitroxide radical. A high rate constant was achieved for both heterogeneous electron transfer ($10^{-1} \text{ cm s}^{-1}$) and homogeneous electron transfer resulting from a self-exchange reaction ($1.8 \times 10^5 \text{ M}^{-1} \text{ s}^{-1}$).³³ Therefore, the PTMA-impregnated CNT seems promising for application to a high-rate sodium battery.

Fig. 4a displays the initial charge-discharge curve of the general PTMA-CNT composite and PTMA-impregnated CNT electrodes for a sodium battery with a 0.1-C rate. During the first charge process, the voltage increases from the OCV to a top cut-off voltage of 4.0 V with one plateau voltage because the start-state involves a nitroxide radical, as shown in Supporting Information Figure S6. However, the first discharge exhibits two plateau voltages for the aminoxy anion with the two-electron process. The initial charge capacity is 61 mAh g⁻¹ for the PTMA-CNT composite and 120 mAh g⁻¹ for the CNT-encapsulated PTMA. During the discharge of the PTMA-CNT composite, the voltage rapidly drops from 4.0 to 1.5 V with a blurred plateau and reaches 142 mAh g⁻¹. On the other hand, the first discharge capacity of the PTMA-impregnated CNT is 222 mAh g⁻¹ and exhibits two notable voltage plateaus at 3.36 V and 2.1 V, corresponding to the two-stage reduction of the oxoammonium cations to nitroxide radicals at the first plateau and of nitroxide radicals to aminoxy anions at the second plateau (Fig. S6, ESI[†]). The change in the PTMA structure during the charge-discharge reaction was monitored by X-ray photoelectron spectroscopy (XPS). The PTMA-impregnated CNT electrodes were carefully disassembled and washed in diethyl carbonate (DEC) and then investigated by XPS. Fig. S7 (ESI[†]) shows the high-resolution XPS core level spectra of Na 1s and N 1s. After the discharge, the intensity of the Na 1s peak increases significantly, indicating Na⁺ uptake with conversion to aminoxy anions upon discharge. The strong peak at 399 eV in the N 1s spectra of the pristine electrode is assigned to the N–O bond of PTMA, while the 402 eV peak

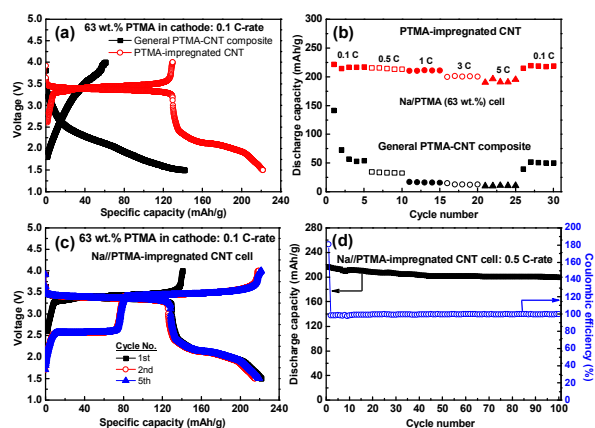


Fig. 4 Initial charge-discharge curves (a) and rate performance (b) of PTMA-CNT composite and PTMA-impregnated CNT electrodes. Potential profiles of charge-discharge at the 1st, 2nd and 5th cycles, and cycle performance of PTMA-impregnated CNT sodium battery at room temperature.

attributed to the N=O bond appears with the formation of the oxoammonium cation upon charging. The XPS results effectively support the two-stage electrochemical reaction of PTMA and demonstrate the possibility of using PTMA with suitably designed high-capacity organic materials for the applications such as sodium batteries. The short cycling performance of Na//PTMA cells with a PTMA-CNT composite electrode and a PTMA-impregnated CNT electrode at different current rates is shown in Fig. 4b. When the current density is increased to 0.1, 0.5, 1, 3, and 5 C, the discharge capacities of the PTMA-impregnated CNT remain at about 222, 216, 210, 200, and 190 mAh g⁻¹, respectively. Therefore, it is clear that the storage capacity of the PTMA-impregnated CNT is stable at each current rate. In contrast, the PTMA-CNT composite exhibits discharge capacities of 142, 35, 17, 15, and 10 mAh g⁻¹ when cycled at different current densities of 0.1, 0.5, 1, 3 and 5 C, respectively. The rate retentions of the PTMA-CNT composite and PTMA-impregnated CNT are 7% and 86%, when the current density increases from 0.1 to 5 C. The fast ion diffusion and rapid electron transfer owing to the interconnected network of the CNT and the enhanced contact between PTMA and the electrolyte result in the high rate performance of the PTMA-impregnated CNT electrode. When the current rate reverses back to 0.1 C in the Na//PTMA-impregnated CNT cell, the cell capacity immediately recovers to its original value, which indicates that the PTMA-impregnated CNT cathode can attain stability even after a high rate of cycling. The charge-discharge curves for the Na//PTMA-impregnated CNT cell appear to be similar for the second and third cycles (Fig. 4c), indicating that the PTMA-impregnated CNT possesses stable charge-discharge properties and good cycle stability. The second charge curve exhibits two voltage plateaus at 2.51 V and 3.51 V, which can be attributed to the two-electron oxidation reaction from aminoxy anions to oxoammonium cations; this result is consistent with CV results

shown in Fig. S8 (ESI[†]). To maintain an appropriate charge balance at the PTMA cathode during the charge-discharge process, the anions/cations in the electrolyte (ClO₄⁻/Na⁺ in the present case) contribute to the redox reaction. The charge and discharge capacities in the second cycle are 219 and 215 mAh g⁻¹, respectively, and it can be seen that the discharge capacity is slightly reduced relative to the first cycle. On the charge-discharge capacity the CNT does not contribute (Fig. S10, ESI[†]). Fig. 4d shows the cycling performance and Coulombic efficiency of the PTMA-impregnated CNT at a rate of 0.5 C. The Na//PTMA-impregnated CNT cell exhibits a high initial discharge capacity of 217 mAh g⁻¹ (230 mAh cm⁻³ volumetric capacity) as well as excellent cycleability with no noticeable decrease in performance, even after 100 cycles. The loss in discharge capacity is less than 8% and the Coulombic efficiency remains close to 100%, with the exception of the first cycle in which the oxidation process starts with the nitroxide radical during the first charge (~190% Coulombic efficiency). Thus, the decrease in overall capacity of the PTMA-impregnated CNT electrode, as calculated from the initial and 100th cycle capacities, is around 0.07% per cycle. In addition, when the PTMA-impregnated CNT was tested as the electrode for lithium battery, it also exhibits promising electrochemical performances as shown in Fig. S11 (ESI[†]). Given its high capacity, excellent cycle stability, high rate capability, and ability to withstand a high load, the PTMA-impregnated CNT can be a promising cathode material for both sodium and lithium batteries. These properties could be attributed to the encapsulation of PTMA in the CNT, which enables easy electrolyte penetration into the inner part of the electrode, while the CNT layer without the insulating PTMA layer could effectively enhance the electrical conductivity and hasten the transport of electrons.

Conclusions

We have successfully prepared a PTMA-impregnated CNT composed of 68 wt.% PTMA and 32 wt.% CNT by means of a dissolution-diffusion-washing process. The PTMA-impregnated CNT was used as an electrode with a 7 wt.% PVdF binder, which enabled the fabrication of sodium batteries with high stability and excellent electrochemical properties. The narrow vacant spaces in the center of the CNT can trap PTMA, preventing the dissolution of the active polymer, self-discharge, and the formation of an insulating PTMA layer on the surface of the electrode and between the CNTs. The PTMA-impregnated CNT electrode also achieves fast ion diffusion by allowing the electrolyte to easily penetrate the electrode and allowing rapid electron transport through the well-connected CNT network without a thick insulating PTMA layer. Therefore, the PTMA-impregnated CNT is beneficial to the enhancement of stability, discharge capacity, cycleability, and rate capability, even with a high PTMA content. The PTMA-impregnated CNT exhibits a reversible redox reaction via a two-electron process. The fabricated electrode was found to deliver an initial discharge capacity of 222-mAh g⁻¹ at a 0.1-C rate, with capacity retention of around 93% after 100 cycles at 0.5 C, thus reflecting the reversible redox nature of the electrode and excellent cycle life. Furthermore, when

measured at high currents, the PTMA-impregnated CNT-electrode also improved the rate capability (210 mAh g⁻¹ at 1 C and 190 mAh g⁻¹ at 5 C). Our results show that the PTMA-impregnated CNT electrode is a very promising candidate for use in sodium batteries with advanced electrochemical properties.

Acknowledgements

This work was supported by the 2015 Research Fund (1.150034.01) of UNIST (Ulsan National Institute of Science and Technology) and Basic Science Research Program through the National Research Foundation of Korea (NRF) funded by the Ministry of Education (NRF-2014R1A1A2A16053515) and (NRF-2014R1A2A1A11052110).

Notes and references

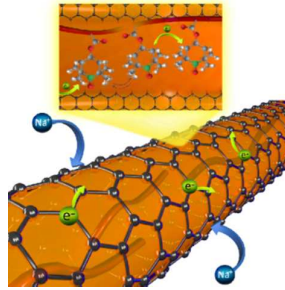
- 1 Y.K. Sun, Z.H. Chen, H.J. Noh, D.J. Lee, H.G. Jung, Y. Ren, S. Wang, C.S. Yoon, S.T. Myung and K. Amine, *Nat. Mater.*, 2012, **11**, 942–947.
- 2 P.G. Bruce, B. Scrosati and J.M. Tarascon, *Angew. Chem. Int. Ed.*, 2008, **47**, 2930–2946.
- 3 N.S. Choi, Z. Chen, S.A. Freunberger, X. Ji, Y.K. Sun, K. Amine, G. Yushin, L.F. Nazar, J. Cho and P.G. Bruce, *Angew. Chem. Int. Ed.*, 2012, **51**, 9994–10024.
- 4 S.W. Kim, D.H. Seo, X. Ma, G. Ceder and K. Kang, *Adv. Energy Mater.*, 2012, **2**, 710–721.
- 5 E. Lee, J. Lu, Y. Ren, X. Luo, X. Zhang, J. Wen, D. Miller, A. DeWahl, S. Hackney, B. Key, D. Kim, M.D. Slater and C.S. Johnson, *Adv. Energy Mater.*, 2014, **4**, 1400458.
- 6 H. Pan, Y.S. Hu and L. Chen, *Energy Environ. Sci.*, 2013, **6**, 2338–2360.
- 7 V. Palomares, P. Serras, I. Villaluenga, K. B. Hueso, J. Carretero-González and T. Rojo, *Energy Environ. Sci.*, 2012, **5**, 5884–5901.
- 8 Y. Liu, Y. Xu, X. Han, C. Pellegrinelli, Y. Zhu, H. Zhu, J. Wan, A.C. Chung, O. Vaaland, C. Wang and L. Hu, *Nano Lett.*, 2012, **12**, 5664–5668.
- 9 S. Wang, L. Wang, K. Zhang, Z. Zhu, Z. Tao and J. Chen, *Nano Lett.*, 2013, **13**, 4404–4409.
- 10 Z. Song, H. Zhan and Y. Zhou, *Angew. Chem. Int. Ed.*, 2010, **49**, 8444–8448.
- 11 M. Stolar and T. Baumgartner, *Phys. Chem. Chem. Phys.*, 2013, **15**, 9007–9024.
- 12 H. Nishid, S. Iwasa, Y. Pu, T. Suga, K. Nakahara and M. Satoh, *Electrochim. Acta*, 2004, **50**, 827–831.
- 13 J.K. Kim, J. Scheers, J.H. Ahn, P. Johansson, A. Matic and P. Jacobsson, *J. Mater. Chem. A*, 2013, **1**, 2426–2430.
- 14 Z. Song and H. Zhou, *Energy Environ. Sci.*, 2013, **6**, 2280–2301.
- 15 W. Guo, Y.X. Yin, S. Xin, Y.G. Guo and L.J. Wan, *Energy Environ. Sci.*, 2012, **5**, 5221–5225.
- 16 Q. Huang, D. Choi, L. Cosimbescu and J. Lemmon, *Phys. Chem. Chem. Phys.*, 2013, **15**, 20912–20928.
- 17 T. Suga, H. Konishi and H. Nishide, *Chem. Commun.*, 2007, 1730–1732.
- 18 Y.H. Wang, M.K. Hung, C.H. Lin, H.C. Lin and J.T. Lee, *Chem. Commun.*, 2011, **47**, 1249–1251.
- 19 J.K. Kim, A. Matic, J.H. Ahn and P. Jacobsson, *RSC Adv.*, 2012, **2**, 9795–9797.
- 20 J.K. Kim, G. Cheruvally, J.H. Ahn, Y.G. Seo, D.S. Choi, S.H. Lee and C.E. Song, *J. Ind. Eng. Chem.*, 2008, **14**, 371–376.

ARTICLE

Journal Name

- 21 M. Kumar and Y. Ando, *J. Nanosci. Nanotechnol.*, 2010, **10**, 3739–3758.
- 22 N. Yan, X. Zhou, Y. Li, F. Wang, H. Zhong, H. Wang and Q. Chen, *Sci. Rep.*, 2013, **3**, 3392; DOI: 10.1038/srep03392.
- 23 J.C. Bachman, R. Kaviani, D.J. Graham, D.Y. Kim, S. Noda, D.G. Nocera, Y. Shao-Horn and S.W. Lee, *Nat. Commun.*, 2015, **6**, 7040; DOI 10.1038/ncomms8040.
- 24 Y. Chen, X. Zhang and Z. Xie, *ACS Nano*, 2015, **9**, 8054–8063.
- 25 M. Kaempgen, C. K. Chan, J. Ma, Y. Cui and G. Gruner, *Nano Lett.*, 2009, **9**, 1872–1876.
- 26 Y.N. Ko, S.B. Park, K.Y. Jung and Y.C. Kang, *Nano Lett.*, 2013, **13**, 5462–5466.
- 27 Y. Shi, J.Z. Wang, S.L. Chou, D. Wexler, H.J. Li, K. Ozawa, H.K. Liu and Y.P. Wu, *Nano Lett.*, 2013, **13**, 4715–4720.
- 28 J.K. Kim, J. Manuel, G.S. Chauhan, J.H. Ahn, H.S. Ryu, *Electrochim. Acta*, 2010, **55**, 1366–1372.
- 29 L. Ji, M. Rao, S. Aloni, L. Wang, E.J. Cairns and Y. Zhang, *Energy Environ. Sci.*, 2011, **4**, 5053–5059.
- 30 J. Guo, Y. Xu and C. Wang, *Nano Lett.* 2011, **11**, 4288–4294.
- 31 A. Manthiram, Y. Fu, S.-H. Chung, C. Zu and Y.-S. Su, *Chem. Rev.*, 2014, **114**, 11751–11787.
- 32 G. He, S. Evers, X. Liang, M. Cuisinier, A. Garsuch, L. F. Nazar, *ACS Nano*, 2013, **7**, 10920–10930.
- 33 K. Nakahara, K. Oyaizu and H. Nishide, *Chem. Lett.*, 2011, **40**, 222–227.

PTMA-impregnated CNT electrode achieves the enhancement of discharge capacity, cycleability and rate capability of sodium battery



Broader context

Sodium (Na) ion batteries attract recently attention as a promising alternative to current lithium ion battery technology for specific applications, such as in electric vehicles, locomotives and energy storage system (ESS) due to their material abundance, low-cost and environmental benignity. Recent researches on Na ion battery are mostly directed on the development of Na intercalated inorganic materials. However, these materials suffer from their low capacity utilization or sluggish kinetics. For this reason, soft materials of the redox-active organic polymers have been investigated as the potential cathodes for Na ion battery due to their advantages over inorganic solids such as open and flexible frame works as well as environmentally friendly. However, organic polymer cathodes suffer from their low electron conductivity and dissolution in the liquid electrolyte, which hinder their use in the commercial battery. To overcome these challenges, the PTMA polymer-impregnated carbon nanotube (CNT) was prepared by dissolution-diffusion-washing process in this work. The well-connected CNT network provides the rapid electron transport in the electrode, and additionally prevents the dissolution of the active polymer into the electrolyte. As a result, the PTMA-impregnated CNT cathode in Na ion battery shows the enhancement of stability, discharge capacity, cycle life, and rate capability.